

Catalyst Behavior in Metal-Catalyzed Carbonyl-Olefin Metathesis

Carly S. Hanson, Mary C. Psaltakis, Janiel J. Cortes, and James J. Devery, III

J. Am. Chem. Soc., **Just Accepted Manuscript** • DOI: 10.1021/jacs.9b02613 • Publication Date (Web): 05 Jul 2019

Downloaded from <http://pubs.acs.org> on July 5, 2019

Just Accepted

“Just Accepted” manuscripts have been peer-reviewed and accepted for publication. They are posted online prior to technical editing, formatting for publication and author proofing. The American Chemical Society provides “Just Accepted” as a service to the research community to expedite the dissemination of scientific material as soon as possible after acceptance. “Just Accepted” manuscripts appear in full in PDF format accompanied by an HTML abstract. “Just Accepted” manuscripts have been fully peer reviewed, but should not be considered the official version of record. They are citable by the Digital Object Identifier (DOI®). “Just Accepted” is an optional service offered to authors. Therefore, the “Just Accepted” Web site may not include all articles that will be published in the journal. After a manuscript is technically edited and formatted, it will be removed from the “Just Accepted” Web site and published as an ASAP article. Note that technical editing may introduce minor changes to the manuscript text and/or graphics which could affect content, and all legal disclaimers and ethical guidelines that apply to the journal pertain. ACS cannot be held responsible for errors or consequences arising from the use of information contained in these “Just Accepted” manuscripts.

Catalyst Behavior in Metal-Catalyzed Carbonyl-Olefin Metathesis.

Carly S. Hanson, Mary C. Psaltakis, Janiel J. Cortes, and James J. Devery, III*

Department of Chemistry & Biochemistry, Loyola University Chicago, Flanner Hall, 1068 W Sheridan Road, Chicago, IL 60660, United States

ABSTRACT: Iron(III)-catalyzed carbonyl-olefin ring-closing metathesis employs reactivity not typically observed in Lewis acid-catalyzed reactions. In converting a ketone with a pendant olefin into a cycloalkene and a simple carbonyl byproduct, the reaction requires the Lewis acid catalyst to differentiate between the carbonyl of the substrate and that of the byproduct. It is necessary to determine how this solution interaction imparts the desired reactivity in order to best employ this method. Herein, we report detailed kinetic, spectroscopic, and colligative measurements applied towards the identification of the solution structures of the active Fe(III) and Ga(III) carbonyl-olefin metathesis catalysts. These data are consistent with formation of Lewis acid-carbonyl pairs for both metal systems under stoichiometric conditions. However, they diverge in the presence of higher equivalents of carbonyl, with Fe(III) forming highly ligated complexes, and no observed change for Ga(III). These findings are consistent with the resting state identity of the Fe(III) metathesis catalyst changing over the course of the reaction.

Introduction

The interactions between Lewis acids and carbonyls have played a significant role in the construction of important molecules.¹ While a great deal of insight has been gained regarding classical stoichiometric regimes, like the Friedel-Crafts reaction, more discoveries continue to be made about the complexities of these interactions between carbonyls and Lewis acids in catalytic systems. In particular, the new reactivity observed in Lewis acid-catalyzed carbonyl-olefin metathesis demonstrates that a comprehensive understanding of the interactions between these classical Lewis pairs remains incomplete. Representing a powerful reaction manifold for the production of C=C bonds from functional groups that are broadly utilized in the construction of complex molecules,² the Fe(III)-catalyzed process developed by Schindler and coworkers³ triggered a series of synthetic developments that expand the use of Fe(III),⁴ employ Ga(III),⁵ I₂,⁶ as well as employing Brønsted acids.⁷ This method has proven useful in the synthesis of many cyclic scaffolds via ring closing, including di- and trisubstituted cyclopentenes and cyclohexenes, polycyclic aromatic hydrocarbons, 2,5-dihydropyrroles, as well as ring-opening metathesis and cross metathesis. One of the major benefits of the transformation is the simplicity of execution, requiring only catalyst, solvent, and a carbonyl-olefin pair: a concise list of variables for mechanistic analysis. However, one question remains unexplored: how does the catalyst distinguish between the substrate carbonyl and product carbonyl? We report herein the solution behavior of the Lewis acid catalyst in the presence of a model substrate and typical carbonyl byproducts. The application of *in situ* infrared spectroscopy displays formation of Lewis acid-dependent aggregates, which competitively inhibit the metathesis cycle. These mechanistic findings provide insight into procedural modifications to facilitate the conversion of recalcitrant metathesis substrates.

Previous efforts from our lab, working alongside the Schindler and Zimmerman labs, focused on the determination

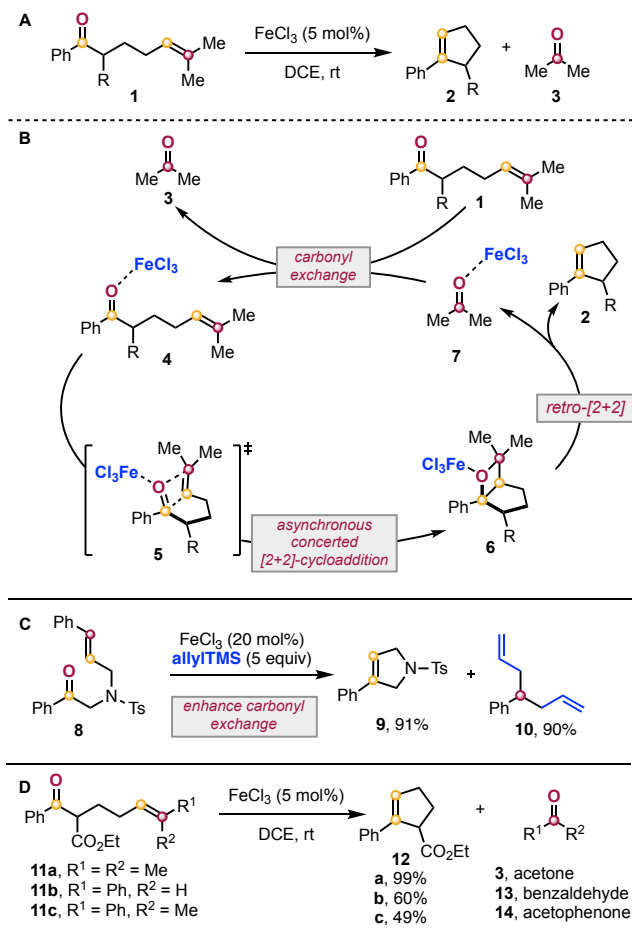


Figure 1. Fe(III)-catalyzed carbonyl-olefin metathesis (A). Catalytic cycle (B). Additive-facilitated metathesis (C). Byproduct-linked diminished yields (D).

of the operating catalytic cycle that results in formation of di-substituted cyclopentene **2** and acetone (**3**, Figure 1A).⁸ We proposed that iron(III) chloride forms coordination complex **4**, resulting in an interaction that activates the carbon-oxygen double bond. The activated complex then undergoes an asynchronous, concerted [2+2]-cycloaddition to form oxetane-complex **5** as the turnover-limiting step. Fe(III)-mediated retro-[2+2] cycloaddition yields cyclopentene **2** and Fe(III) complex (**7**). Carbonyl exchange allows for the subsequent catalytic turnover.

The final step of the cycle is critical for the success of the catalytic mechanism, suggesting that product inhibition is likely, under reaction conditions. Indeed, Li and coworkers reported the use of an additive to facilitate the formation of dihydropyrroles (**9**) from *N*-cinnamyl glycine derivatives (**8**, Figure 1C).^{4a} Utilizing a styrenyl olefin partner that results in the formation of benzaldehyde as the carbonyl byproduct, they observed that product formation required the addition of superstoichiometric allyltrimethylsilane. This additive facilitated the formation of the desired heterocycle, as well as diallylated **10**.⁹ Similarly, we observed that systems that formed benzaldehyde or acetophenone as the byproduct provided diminished yields (Figure 1D). In addition to these potential effects of byproduct, we have also demonstrated that the addition of exogenous Lewis bases to the reaction mixture eliminates metathesis reactivity.⁸ Further, Schindler, Zimmerman, and coworkers showed that Lewis basic moieties within the substrate have the potential to inhibit the preferred reactivity.^{4c} These collected observations are consistent with byproduct inhibition occurring via inefficient carbonyl exchange.

Results and Discussion

Kinetic Analysis: Our initial efforts to elucidate the presence of byproduct inhibition began with observation of the metathesis reaction under synthetically relevant conditions. Using the reaction defined in Figure 2A, we employed aromatic ketone **15** as the substrate for the metathesis reaction in DCE.¹⁰ The extraction of kinetic information occurred by monitoring the [15] via reversed-phase ultra-performance liquid chromatography coupled with a transmission UV/vis detector. We performed reactions by first combining a metal halide with DCE. Then, catalysis was initiated via the addition of **15** to the mixture. To obtain a baseline for this particular reaction, we examined an FeCl₃-catalyzed system (■, Figure 2B), as well as a GaCl₃-catalyzed system (●, Figure 2B). The Fe(III) reaction displays a significantly faster rate than Ga(III), as we have previously reported.⁸

Next, we initiated the reaction in the presence of 0.5 equiv **3** with respect to **15**. This modification was accomplished by pre-mixing **3** with the salt/DCE slurry prior to addition of **15**. In the presence of 0.5 equiv added byproduct **3**, we observe significant inhibition of catalytic activity for the Fe(III)-mediated system, decreasing the reaction to a rate slower than the GaCl₃ process. Similarly, we observe a decrease in rate when the GaCl₃-catalyzed reaction is initiated in the presence of **3**; however, the decrease is less significant compared to that observed when Fe(III) is employed. We continued our examination of the impact of **3** on the rate of reaction, probing 0.2 equiv **3** with respect to **15**.¹¹ In both systems, we observe a concentration-dependent deleterious effect on the rate of reaction arising from the presence of **3**; however, in neither case is this decrease consistent with a whole number rate order. Collectively, these data are consistent with catalyst behavior being impacted by the identity of the Lewis acid. Under typical reaction conditions for **15**, Fe(III) is a much more efficient catalyst. However, its rate is significantly

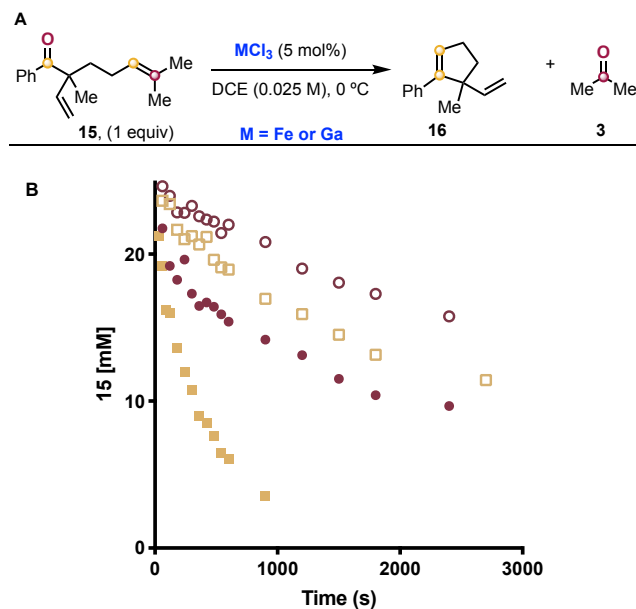


Figure 2. Metal halide-catalyzed carbonyl-olefin metathesis of **15** (A) FeCl₃-mediated system (■), GaCl₃-system (●), FeCl₃-mediated system with 0.5 equiv **3** (□), GaCl₃-mediated system with 0.5 equiv **3** (○) (B) Error bars omitted for clarity.¹¹

impacted by the presence of byproduct compared to Ga(III). Intriguingly, the slopes of the decays suggest that the Ga-catalyzed system appears to approach a constant rate whether or not the reaction is initiated in the presence of **3**; whereas, this observation is not present in the Fe reaction, suggesting different affinities for the interactions of Fe and Ga with **3** and **15**.

Spectroscopic Investigation: The contrasting observations we confronted for the FeCl₃- and GaCl₃-catalyzed systems necessitated an in-depth examination of the interactions of these catalysts with carbonyls. These interactions have played a significant role in the construction of important molecules.¹ Because of their widespread application, significant effort has been devoted to characterizing the behavior of Lewis acids and bases, relying heavily on infrared (IR) spectroscopy to elucidate the discrete structure of Lewis pairs, and to utilize IR as a tool for the determination of Lewis acidity.^{1d,12} In particular, the Susz lab studied the stoichiometric coordinating interactions of Lewis acids and carbonyls in great detail in the solid state. They employed IR and elemental analysis to determine the composition of neat, 1:1 mixtures of Lewis pairs, yielding a great deal of structural information about the interactions of simple ketones and aldehydes with a range of Lewis acids. These data form a solid foundation for the spectroscopic behavior of **3**, benzaldehyde (**13**), and acetophenone (**14**) in the presence of AlCl₃,¹³ TiCl₄,¹⁴ BF₃,¹⁵ and FeCl₃.¹⁵

With this wealth of spectroscopic information in the solid state available as a starting point, we began to examine the solution interactions of GaCl₃ and FeCl₃ in combination with **3**, **13**, and **14**. Using solution IR, we posited that we would be able to compare the relative amounts of free carbonyl compound with the complex formed between the carbonyl and Lewis acid. Under anhydrous conditions, GaCl₃ and FeCl₃ have very different solubilities, with GaCl₃ rapidly dissolving and FeCl₃ being largely insoluble in DCE. We prepared mixtures of these salts to which we titrated carbonyl incrementally. Our spectroscopic investigation began with the examination of the interaction between GaCl₃ and **3**. Intriguingly, between 0 and 1 equiv **3** added to the solution, we observe no unbound **3**. In the carbonyl region

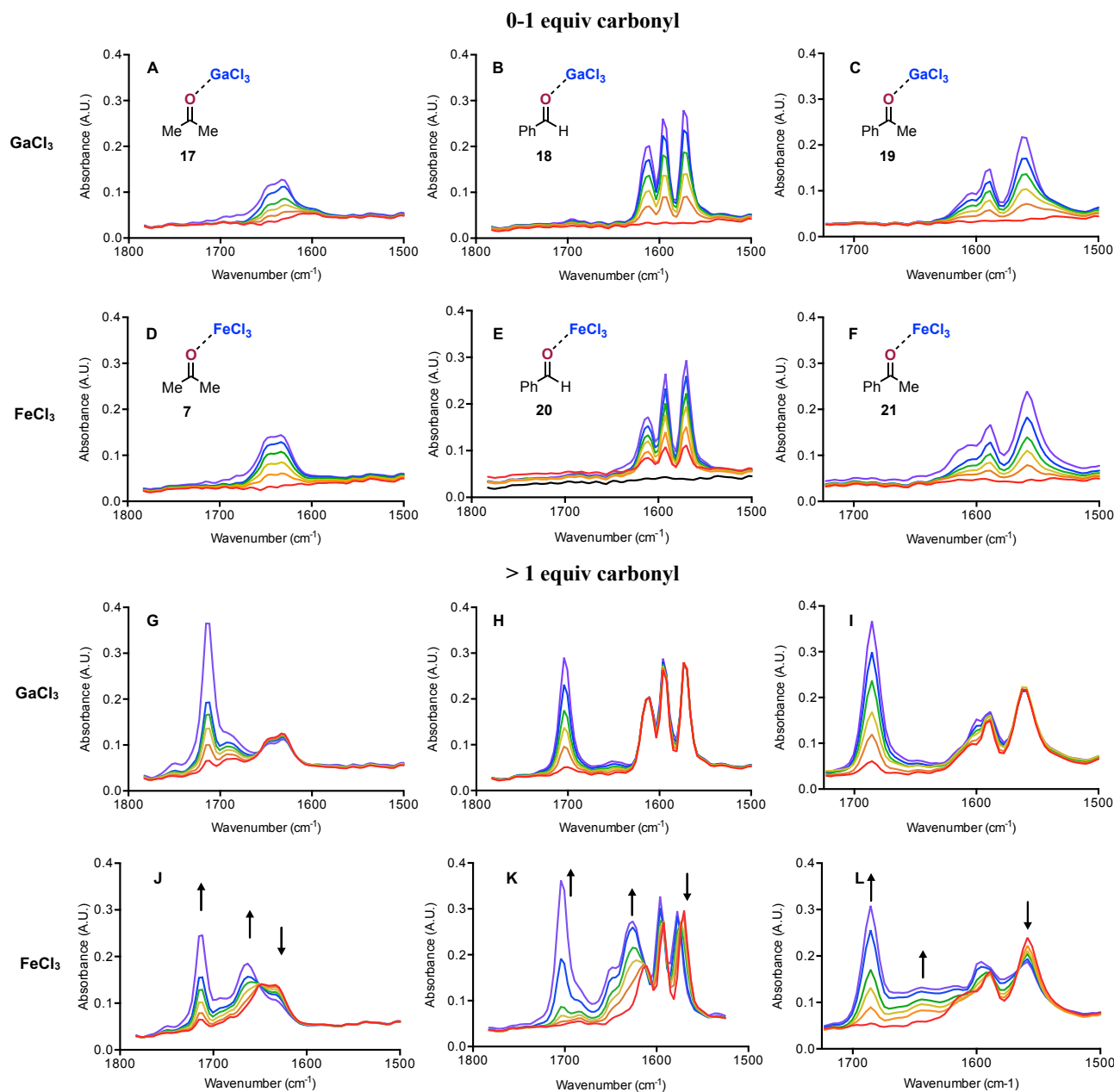


Figure 3. Solution IR data for titrations of GaCl₃ (1 mmol in 6 mL DCE) and FeCl₃ (2 mmol in 12 mL DCE) with 0-1 equiv **3** (A and D), **13** (B and E), and **14** (C and F), as well as >1 equiv **3** (G and J), **13** (H and K), and **14** (I and L). Titrations proceed from red to violet with increasing amounts of titrant. (A: [**3**] = 0 M, 0.023 M, 0.045 M, 0.067 M, 0.112 M, 0.156 M. B: [**13**] = 0 M, 0.049 M, 0.081 M, 0.097 M, 0.129 M, 0.160 M. C: [**14**] = 0 M, 0.029 M, 0.057 M, 0.085 M, 0.113 M, 0.155 M. D: [**3**] = 0 M, 0.034 M, 0.067 M, 0.101 M, 0.134 M, 0.178 M. E: [**13**] = 0 M, 0.033 M, 0.057 M, 0.081 M, 0.105 M, 0.129 M, 0.161 M. F: [**14**] = 0 M, 0.021 M, 0.043 M, 0.071 M, 0.113 M, 0.168 M. G: [**3**] = 0.222 M, 0.287 M, 0.351 M, 0.415 M, 0.499 M, 0.786 M. H: [**13**] = 0.177 M, 0.224 M, 0.270 M, 0.316 M, 0.392 M, 0.482 M. I: [**14**] = 0.196 M, 0.277 M, 0.343 M, 0.473 M, 0.599 M, 0.721 M. J: [**3**] = 0.233 M, 0.265 M, 0.319 M, 0.383 M, 0.447 M, 0.593 M. K: [**13**] = 0.177 M, 0.224 M, 0.270 M, 0.316 M, 0.541 M, 0.824 M. L: [**14**] = 0.182 M, 0.263 M, 0.330 M, 0.460 M, 0.523 M, 0.586 M).¹¹

of the spectrum, we observe exclusive formation of a signal at 1630 cm⁻¹ (Figure 3A). When a similar titration was performed with FeCl₃, again no unbound **3** was observed, with exclusive formation of a vibration at 1633 cm⁻¹ (Figure 3D). Importantly, the FeCl₃ system remains heterogeneous until 1 equiv **3** is present. We performed an analogous titration with **13** and GaCl₃ and observed exclusive formation of a single species with absorbances at 1610, 1596, and 1573 cm⁻¹ (Figure 3B). The corresponding titration into an FeCl₃ slurry resulted in the formation of a species with vibrations at 1610, 1592, and 1569 cm⁻¹ (Figure 3E). Again, the FeCl₃ system remains heterogeneous until 1 equiv **13** is present in solution with respect to metal halide.

When the titrant is **14**, GaCl₃ yields 1603, 1588, and 1563 cm⁻¹ (Figure 3C), while FeCl₃ provides 1603, 1589, and 1558 cm⁻¹ (Figure 3F). The presence of 1 equiv **14** with respect to FeCl₃ generates a homogeneous solution.

In their study of the interactions of Lewis acids and bases, the Susz lab prepared a number of 1:1 complexes of Lewis acids and carbonyls as solids. They examined these structures via elemental analysis to determine their composition and IR to determine the manner of interaction between acid and base. They report a 1:1 complex between **3** and BF₃ (1640 cm⁻¹),^{15a} as well as with **3** and TiCl₄ (1625 cm⁻¹).^{14b} Further, Greenwood measured the heat of formation of a 1:1 GaCl₃-**3** complex at -15.3

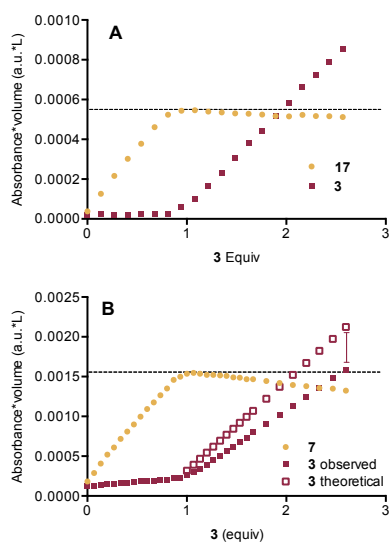


Figure 4. Analysis of components: **3** and **17** (A) as well as **3**, theoretical **3** after 1 equiv, and **7** (B).¹¹

kcal mol⁻¹,¹⁶ consistent with our observed absence of unbound **3**. These precedents are consistent with our observations between **3** and both GaCl₃ and FeCl₃, suggesting that between 0 and 1 equiv **3**, a 1:1 coordination complex forms exclusively between **3** and GaCl₃ (**17**), as well as **3** and FeCl₃ (**7**). The similar behavior observed in the systems employing **13** and **14** is suggestive of an analogous complexation, where **13** forms benzaldehyde-GaCl₃ complex **18** and benzaldehyde-FeCl₃ complex **20**. The corresponding addition of **14** forms acetophenone-GaCl₃ complex **19** and acetophenone-FeCl₃ complex **21** with GaCl₃ and FeCl₃, respectively. Our observation of **21** is consistent with the solid state IR reported by the Susz lab.^{15b} Further, Kochi and coworkers reported a crystal structure of an analogous GaCl₃ complex with 4-fluorobenzoyl chloride.¹⁷

Interestingly, when the addition of the carbonyl proceeds beyond 1 equiv with respect to the metal halide, the behavior of the two systems diverges. For GaCl₃, when >1 equiv **3**, **13**, and **14** are added to the solution, we observe the presence of unbound carbonyl: 1714 cm⁻¹ for **3** (Figure 3G), 1704 cm⁻¹ for **13** (Figure 3H), and 1685 cm⁻¹ for **14** (Figure 3I). When this same range of **3** is added to FeCl₃, more complex spectra are obtained.

When **3** is added beyond 1 equiv, we observe an isosbestic point at 1648 cm⁻¹ (Figure 3J). The C=O vibration of free **3** is observed at 1714 cm⁻¹; however, we also observe the signal at 1644 cm⁻¹ decrease in intensity while a new signal at 1663 cm⁻¹ forms. Similarly, when **13** is added beyond 1 equiv, an isosbestic point is observed at 1574 cm⁻¹ (Figure 3K). Simultaneously, as the intensity of the signal for free **13** grows (1704 cm⁻¹), the signal at 1569 cm⁻¹ decreases while 1577 cm⁻¹ and 1626 cm⁻¹ grow. For the addition of superstoichiometric **14** to FeCl₃, an isosbestic point is present at 1566 cm⁻¹ (Figure 3L). The vibration for **21** at 1558 cm⁻¹ decreases as more **14** is observed at 1685 cm⁻¹. Further, the range between 1670 and 1610 cm⁻¹ grows.

To gain more insight into the difference in behavior of GaCl₃ and FeCl₃, we examined the amounts of each component present in solution with respect to the equivalents of carbonyl added. Because data are collected via titration, dilution is a factor for which we must account. We accomplish this task through normalization of the absorbance of the λ_{max} of each component (**3** = 1714 cm⁻¹, **7** = 1644 cm⁻¹, **13** = 1704 cm⁻¹, **14** = 1685 cm⁻¹, **17** = 1633 cm⁻¹, **18** = 1573 cm⁻¹, **19** = 1563 cm⁻¹, **20** = 1569 cm⁻¹

¹, **21** = 1558 cm⁻¹) by multiplying the signal by the volume present in each measurement yielding eq. 1:

$$AV = \epsilon ln \quad (1)$$

where 1) both absorbance (A) and volume (V) are measurable terms; 2) molar absorptivity (ε) and pathlength (l) are constant, allowing 3) number of moles (n) to be examined. Using eq. 1, we can examine the observed amount of each component as a function of equivalents of carbonyl added (Figure 4).

When we consider the addition of **3** to GaCl₃, we see several key observations (Figure 4A). The amount of **17** (●) increases proportionately with the amount of **3** from 0 equiv **3** until ≈1 equiv **3** has been added. After an equivalent amount of **3** with respect to GaCl₃ is present, no significant change in amount of **17** occurs, concomitant with observation of **3** in solution (■). Analogous features are observed for the addition of **13** to GaCl₃ and **14** to GaCl₃.¹¹ Similarly, the titrations of carbonyls into the FeCl₃ mixture display proportional growth in the amount of **7** (Figure 4B), **20**, and **21**.¹¹ In all three cases, the amount of 1:1 Lewis acid-carbonyl complex increases until 1 equiv carbonyl is present in solution. However, after the addition of 1 equiv carbonyl, the Fe-containing systems diverge from their Ga-containing counterparts. In all three cases, the amount of coordination complex decreases with increasing equivalents of carbonyl.

At this point, it is important to consider our collected observations from all six titrations. 1) Under anhydrous conditions, GaCl₃ is soluble in DCE while FeCl₃ is not. 2) The solubility of FeCl₃ increases with increasing amount of added carbonyl, regardless of identity. 3) Upon the addition of 1 equiv carbonyl, all three Fe systems achieve homogeneity. 4) Solution IR of all six systems displays vibrations consistent with the formation of 1:1 Lewis acid-carbonyl coordination complexes, similar to the IR spectra reported by Susz for identical/analogous structures. 5) In all cases, no uncoordinated carbonyl is observed until the first equivalence point is reached. Collectively, these observations suggest that, beginning at 1 equiv carbonyl added, the signal of uncoordinated titrant should be representative of the total amount added. The amounts of **3**, **13**, and **14** observed in each of the titrations are consistent with this statement, suggesting that once each GaCl₃ molecule is ligated by a molecule of carbonyl, no further measurable interaction occurs. Alternatively, the suggestion that all carbonyl added after the equivalence point should be observable does not hold true for the FeCl₃ systems. When the titration of FeCl₃ with **3** is considered, we know what the signal of **3** should be based on observation in the absence of FeCl₃ (Figure 4B).¹¹ The amount of **3** observed (■) is less than expected (□). This observation is similarly true for the observed amounts of **13** as well as the observed amounts of **14**.¹¹ When these observations are taken in context with our data that include the formation of new spectral features concomitant with decrease in the intensity of coordination complex, they suggest that **7**, **20**, and **21** are being consumed and converted to alternate complexes.

For the FeCl₃ systems, once the equivalence point is reached, the amount of 1:1 coordination complex decreases with increasing equivalents of carbonyl. The data presented so far are consistent with the amount of carbonyl added being equivalent to the amount of 1:1 coordination complex formed for the titration range from 0 to 1 equiv carbonyl. Additionally, the maximal amount of complex is defined by the moles of metal halide present (C_{MAX} = 2 mmol FeCl₃). With this relationship, we can treat the moles of carbonyl added (C_{ADD}) as equal to the moles of coordination complex (C_{COORD}) to develop a Beer-Lambert relationship with absorbance.¹¹ We can use this relationship

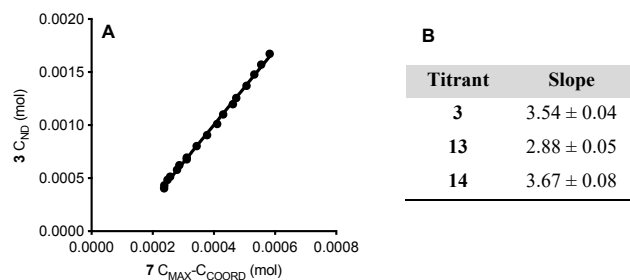


Figure 5. Undetected carbonyl C_{ND} vs. consumed coordination complex for **3** and **7** (A), and the slopes of the correlations for **3** and **7**, **13** and **20**, as well as **14** and **21** (B).¹¹

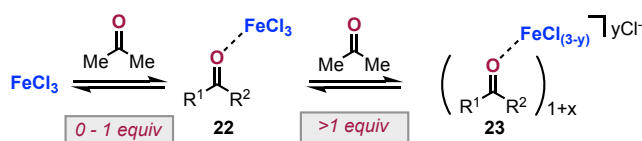


Figure 6. Proposed solution behavior of FeCl_3 in the presence of carbonyl byproducts in DCE.

observed in the 0-1 equiv region to determine C_{COORD} for observations >1 equiv carbonyl via absorbance. This amount can be compared to the theoretical amount of complex to determine the amount consumed by excess carbonyl. Additionally, some amount of the carbonyl added is not detected spectroscopically as either C_{COORD} or unbound (C_{OBS}). Specifically, we can track the as yet undetected carbonyl in the mass balance in eq. 2:

$$C_{ADD} = C_{OBS} + C_{COORD} + C_{ND} \quad (2)$$

where C_{ND} is the moles of carbonyl not detected. Using the region >1 equiv carbonyl added, we can plot C_{ND} as a function of the moles of complex that have been consumed ($C_{MAX} - C_{COORD}$). Indeed, when these values are compared, we observe a linear relationship between the moles of undetected carbonyl and the moles of coordination complex **7** that have been consumed (Figure 5). We observe correlation between the amount of carbonyl for which we cannot account and the amount of complex that is consumed with similar results for **13** and **14**.¹¹ Importantly, both axes have units in moles, suggesting that the slope of the line is related to the moles of carbonyl necessary to consume one mole of 1:1 Lewis acid-carbonyl coordination complex. The relationship between **3** and **7** suggests that 3-4 equiv **3** are required to consume 1 equiv **7** (Figure 5). Similar analysis of **13** suggests that ≈ 3 equiv **13** are required to consume 1 equiv **20**, and the relationship between **14** and **21** suggests that 3-4 equiv **14** are required to consume 1 equiv **21**.¹¹

If we consider the structural ramifications of the correlations in Figure 5, they collectively provide a great deal of insight into the solution behavior of FeCl_3 in the presence of carbonyls. When FeCl_3 is exposed to a stoichiometric amount of carbonyl compound, the classical solution structures for Lewis-acid-mediated systems form, comprised of one molecule of FeCl_3 and one molecule of carbonyl compound (**22**, Figure 6). However, in the presence of a superstoichiometric amount of carbonyl, complexes form via the addition of further equivalents of carbonyl compounds. As a result, some population of carbonyl-ligated complexes will exist in solution with different degrees of coordination by the carbonyl (**23**). When x is consistent with the slopes observed in Figure 5 (slope ≥ 3), this process will form structures where some number (y) of the chloride ligands are displaced to the outer sphere. If this process is occurring, one or more colligative properties of the solution will change.

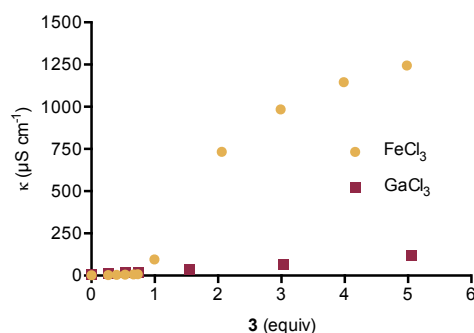


Figure 7. Conductivity of FeCl_3 (2 mmol in 12 mL DCE) and GaCl_3 (2 mmol in 12 mL DCE) with increasing amounts of **3**.¹¹

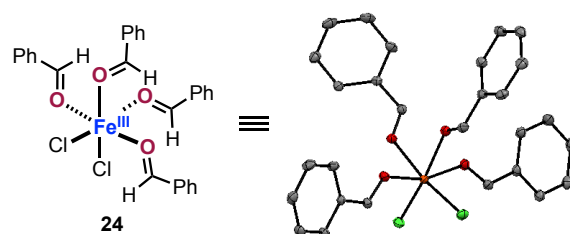


Figure 8. Solid state structure of **24**. Thermal ellipsoids at 50% probability; hydrogen atoms and counter anions (FeCl_4^-) omitted for clarity. Color key: orange = Fe, red = O, gray = C, green = Cl.¹¹

Further, detailed ^{71}Ga NMR experiments by Novikov, Tomilov, and coworkers show the addition of three chelating ligands to a Ga(III) center, resulting in the formation of ion pairs.¹⁸ If our GaCl_3 systems behave analogously, we should observe the effects of ion pair formation.

Colligative Measurements: To probe the interactions of FeCl_3 and GaCl_3 in DCE with superstoichiometric amounts of **3**, **13**, and **14**, we examined the conductivity (κ) with increasing amounts of carbonyl (Figure 7). These measurements were accomplished via titration using identical concentrations to those employed for our IR investigation. Beginning with GaCl_3 and **3** (■, Figure 7A), we see a slight increase in κ from 0-5 equiv **3** to a value of 121 $\mu\text{S cm}^{-1}$. For FeCl_3 and **3** (●), we see analogous behavior from 0-1 equiv added **3**. At the equivalence point, we see a conductivity of 96 $\mu\text{S cm}^{-1}$ for the FeCl_3 system. At 2 equiv **3**, κ increases to 733 $\mu\text{S cm}^{-1}$, which continues up to 1244 $\mu\text{S cm}^{-1}$ at 5 equiv **3**. We obtained analogous results for titrations of **13** and **14**. Titration of GaCl_3 with **13** displays little increase in κ over the course of the titration, achieving a value of 59 $\mu\text{S cm}^{-1}$ at 5 equiv **13**. The addition of **13** to FeCl_3 displays negligible conductivity from 0-1 equiv **13**, while rapidly increasing to 1247 $\mu\text{S cm}^{-1}$ at 2 equiv **13**. Lastly, examination of the combination of both metal halides with **14** yields results proximal to the titrations with **3**. The GaCl_3 titration displays a marginal increase in conductivity; whereas, the addition of **14** to FeCl_3 achieves a κ of 796 $\mu\text{S cm}^{-1}$ at 2 equiv **14**, which increases to 1223 $\mu\text{S cm}^{-1}$ at 5 equiv added **14**.

Detailed examination of these results yields several key insights. We continue to observe analogous behavior between the GaCl_3 systems and the FeCl_3 systems for <1 equiv added carbonyl. Similar to IR, the behavior of both systems diverge upon the addition of ≥ 1 equiv carbonyl, with GaCl_3 displaying marginal if not negligible changes in properties, while FeCl_3 displays properties consistent with the formation of ion pairs ($x \geq 3$ and $y \geq 1$, Figure 6). Importantly, the observed behavior is inconsistent with the complexes reported by Novikov, Tomilov, and

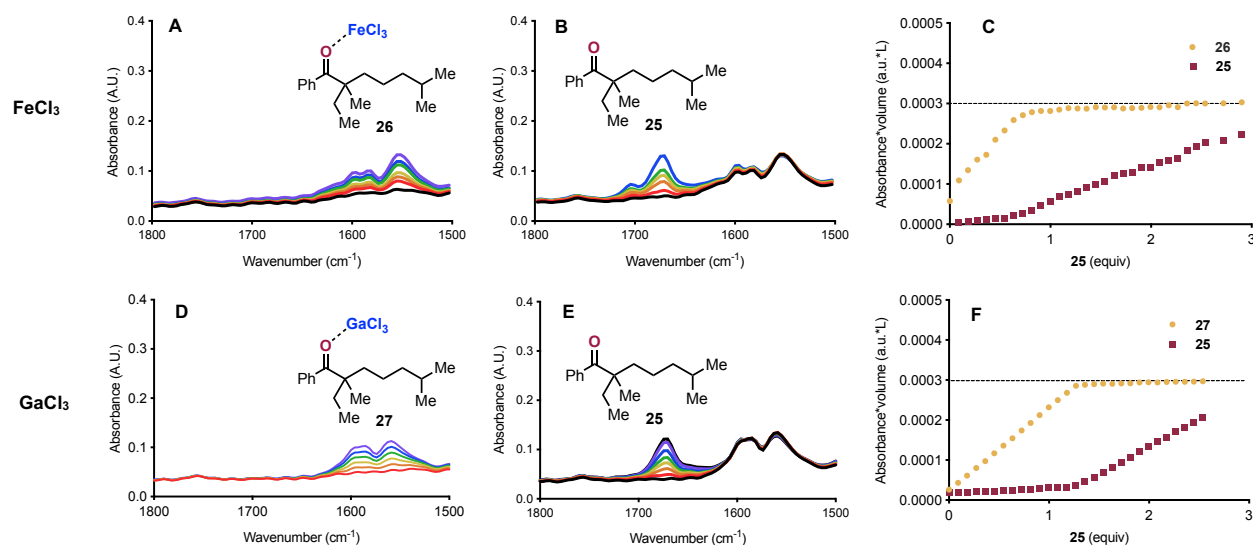


Figure 9. Solution IR data for titrations of FeCl₃ (0.5 mmol in 3 mL DCE) and GaCl₃ (0.5 mmol in 3 mL DCE) with 0-1 equiv **25** (A and D), as well as >1 equiv **25** (B and E). Titrations proceed from red to violet with increasing amounts of titrant. Analysis of components: **25** and **26** (C); **25** and **27** (F). (A: [**25**] = 0 M, 0.015 M, 0.030 M, 0.045 M, 0.074 M, 0.089 M, 0.132 M. B: [**25**] = 0.146 M, 0.202 M, 0.310 M, 0.361 M, 0.437 M, 0.580 M. D: [**25**] = 0 M, 0.030 M, 0.060 M, 0.089 M, 0.118 M, 0.146 M. E: [**25**] = 0.202 M, 0.243 M, 0.283 M, 0.323 M, 0.361 M, 0.486 M, 0.510 M).¹¹

coworkers, suggesting that displacement of the counterions from Ga(III) may require chelating carbonyl ligands.¹⁸

Crystallographic Investigation: To gain further support for the solution structures that are possible in the reaction in Figure 2A, we turned to X-ray crystallography.¹⁹ Indeed, when FeCl₃ is combined in DCE in the presence of excess **13** with pentane-assisted precipitation, we are able to resolve a crystal structure for FeCl₃ (**24**, Figure 8).¹¹ We observe an octahedral, Fe-centered complex, showing that **13** displaces one chloride anion in **24**. Importantly, the observed number of molecules of **13** bound to the Fe(III) center is consistent with our analysis in Figure 5, where three additional equivalents of **13** add to complex **20**. The presence of four molecules of **13** as well as two chloride anions is consistent with our conductance data, where solution conductivity increases because of displacement of chloride to the outer sphere. This higher order of coordination is consistent with Denmark and coworkers' report on interactions of SnCl₄ with aldehydes.²⁰ It is important to point out that this structure represents a single possible coordination complex in this system, and that it is simply the structure that precipitates under forcing conditions. Further, we do not observe precipitation under reaction or titration conditions, and our titration data are consistent with complete formation of 1:1 coordination complex followed by subsequent addition to form a more highly ligated species.

Taken together, these observations suggest that the FeCl₄⁻ observed in the crystal structure is an artifact of the equilibria involved in precipitation. In order to form FeCl₄⁻ in our titrations, 2 equiv byproduct would be required to consume 2 equiv 1:1 complex (1 mol **13** per 1 mol **20**). Our analysis in Figure 5 is consistent with 3 equiv of byproduct consuming 1 equiv 1:1 complex (3 mol **13** per 1 mol **20**). Lastly, formation of FeCl₄⁻ could be consistent with the superelectrophilic homo dimers reported by Schindler, Sigman, and Zimmerman.^{4e} In their report, they observe second order kinetics with respect to FeCl₃ when employing aliphatic ketones as substrates; whereas, aromatic ketones display first order kinetics with respect to FeCl₃, which is inconsistent with the superelectrophile-mediated process. Examination of the rate order of FeCl₃ for the reaction of aromatic

ketone **15** displays an order of 1.13 ± 0.03 ,¹¹ which is consistent with other reports on reactions of aromatic ketones.^{4e,8}

Substrate Analysis: Having characterized the interactions of typical carbonyl-olefin metathesis byproducts in detail, we next examined the interactions of substrate and metal halide. Because of the rapidity of reaction onset when either FeCl₃ or GaCl₃ are combined with **15**, we examined the Lewis acid-carbonyl interactions of **25**: the structural analogue of the substrate, but with the olefin partner hydrogenated.¹⁶ We applied our titration protocol to this model and found little difference in behavior between the Fe(III) and Ga(III) systems (Figure 9). Between 0 and 1 equiv **25** added to the solution, we observe no unbound **25** in either system, consistent with our observations for simple carbonyls. In the carbonyl region of the Fe(III) spectrum, we observe the formation of signals at 1551, 1584, and 1596 cm⁻¹ (Figure 9A). Again, the FeCl₃ system remains heterogeneous until 1 equiv **25** is present. Equivalent spectroscopic features are present with GaCl₃, with formation of vibrations at 1558 and 1584 cm⁻¹ (Figure 9D). Interestingly, when the addition of **25** proceeds beyond 1 equiv, we no longer observe the divergent behavior seen with simple carbonyls (Figures 9B and 9E). In both systems, the initial vibrations remain unchanged at higher equivalents of **25**, and we observe the carbonyl of **25** at 1670 cm⁻¹. These spectral features can be seen in greater clarity via analysis of the system components (Figures 9C and 9F). In both systems, we observe growth of the coordination complex to a maximum at approximately 1 equiv **25**, at which point **25** is observed. The appearance of **25** at lower equivalents in Figure 9C suggests a different binding affinity between the substrate and FeCl₃ and the substrate and GaCl₃. Importantly, highly ligated complexes are not observed.

Carbonyl Exchange: Lastly, we sought to examine the ability of the substrate to displace byproduct in order to access the Fe-center in the carbonyl exchange step. To this end, we performed a titration, in which we preformed 1:1 complex **7**, and then added increasing amounts of **25**. When **25** is added to **7** from 0-1 equiv, **7** is consumed, free **3** appears, free **25** can be observed, as well as 1:1 complex **26** (Figure 10A). When **25** is added from

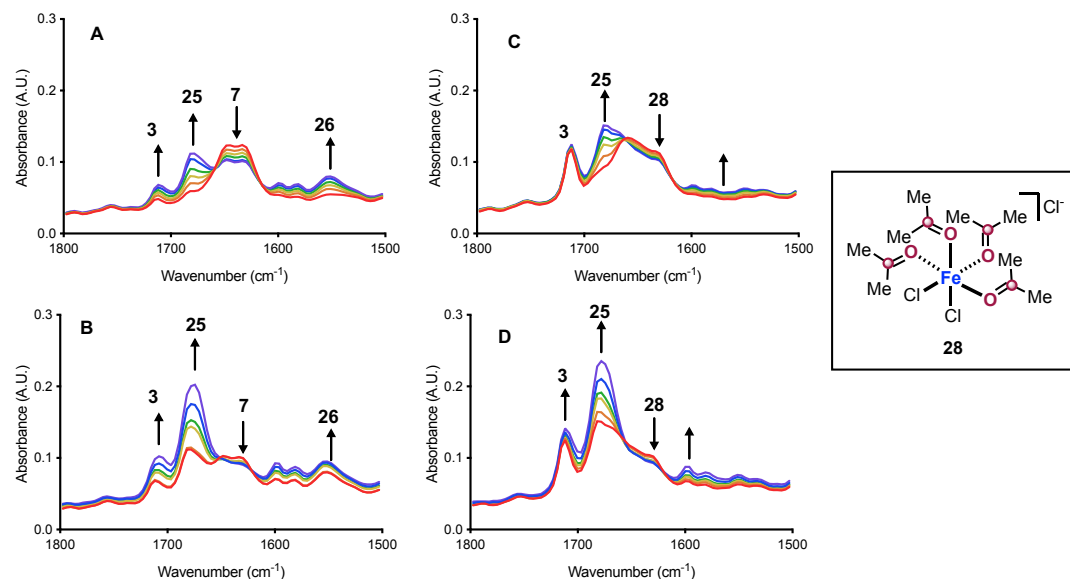


Figure 10. Solution IR data for titrations of 1:1 acetone-FeCl₃ (0.5 mmol in 3 mL DCE) with 0-1 equiv **25** (A) as well as >1 equiv **25** (B). Solution IR data for titrations of 2:1 acetone-FeCl₃ (0.5 mmol in 3 mL DCE) with 0-1 equiv **25** (C), as well as >1 equiv **25** (D). Titrations proceed from red to violet with increasing amounts of titrant. (A: [**25**] = 0 M, 0.045 M, 0.074 M, 0.103 M, 0.123 M, 0.174 M. B: [**25**] = 0.202 M, 0.257 M, 0.323 M, 0.374 M, 0.474 M, 0.591 M. C: [**25**] = 0 M, 0.045 M, 0.074 M, 0.103 M, 0.131 M, 0.174 M. D: [**25**] = 0.201 M, 0.256 M, 0.321 M, 0.373 M, 0.471 M, 0.589 M).¹¹

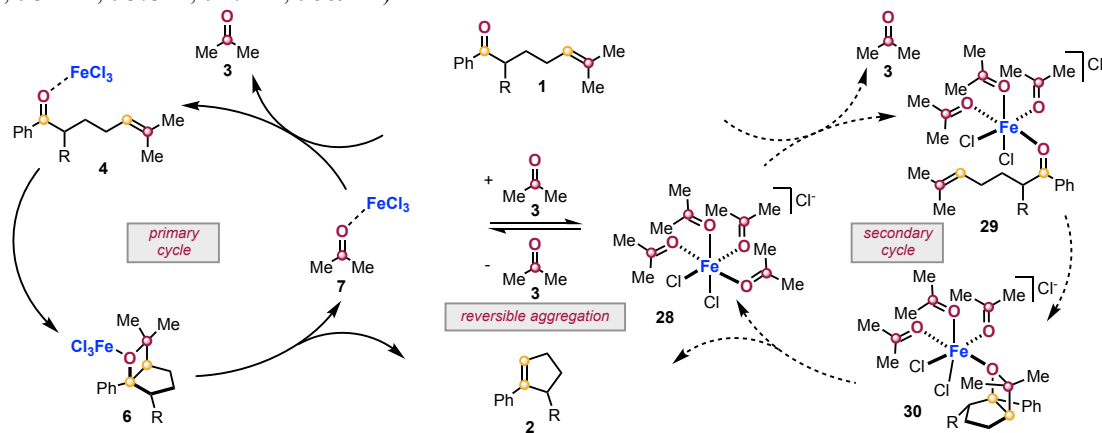


Figure 11. Final mechanistic proposal.

1-3 equiv, more **26** is formed, more **7** is consumed, and more free **3** and free **25** are observed (Figure 10B). These data suggest that the substrate is capable of displacing the byproduct present in 1:1 byproduct complex **7** to form 1:1 substrate complex **26**.

We observe disparate behavior when the titration begins with highly ligated byproduct complex **28**. When **25** is added to this complex from 0-1 equiv, the most significant change in the spectrum is an increase in the signal for unbound **25** (Figure 10C). There are minimal changes in the intensity of **28**, trace amounts of **26** are observed, and the signal for free **3** remains unchanged. When **25** is added from 1-3 equiv, again, the most significant change is the addition of unbound **25**. A small increase in free **3** is present, and a few vibrations appear in the region where 1:1 complex **26** appears. However, the λ_{max} in this region is not consistent with the signal observed in Figure 9A, and may represent a different structure. Lastly, we can explain the behavior of the FeCl₃ catalyst as the reaction progresses with these data. At low conversion, Figure 10B represents the system at high concentration of substrate and low concentration of byproduct. Whereas, Figure 10C represents catalyst conditions from 50% conversion to termination, resulting in **28**.

Alternatively, when the reaction is initiated with 0.5 equiv **3** with respect to substrate, the reaction begins at 10D, with far less substrate able to bind exclusively to FeCl₃. This shift in Fe structure to the highly ligated system coincides with decrease in rate and even termination of reactivity.

Final Mechanistic Proposal: Our kinetic, spectroscopic, conductance, and crystallographic investigations yield the following results: 1) The rate of catalytic turnover is decreased by the byproduct when FeCl₃ is the catalyst. 2) This interaction in the GaCl₃ system is not nearly as pronounced. 3) Titration of both GaCl₃ and FeCl₃ in DCE with 0-1 equiv **3**, **13**, and **14** all result in exclusive formation of a 1:1 Lewis acid-carbonyl coordination complex, consistent with previous reports. 4) When >1 equiv **3**, **13**, or **14** are added to GaCl₃, no effect is detected spectroscopically or via conductance. 5) When >1 equiv **3**, **13**, or **14** are added to FeCl₃, the initial complex is consumed and is converted to an alternative species detected by IR, consistent with the addition of ≥ 3 additional equivalents of carbonyl compound. 6) When FeCl₃ in DCE is exposed to >1 equiv of **3**, **13**, or **14**, a marked increase in conductivity is observed, consistent with the formation of solvent-separated ion pairs. 7) X-ray

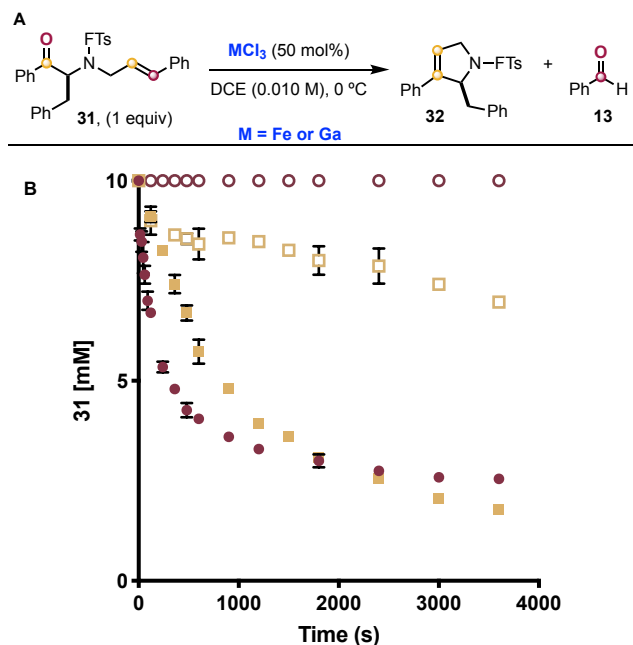


Figure 12. Metal halide-mediated carbonyl-olefin metathesis of **31** (A). GaCl₃-mediated system (●), FeCl₃-mediated system (■), 1:1 **13**:FeCl₃-mediated (□), 1:1 **13**:GaCl₃-mediated system (○) (B).¹¹

crystallographic data demonstrate that an octahedral Fe-centered complex can form in solution and displace the original chloride ligands. 8) The highly ligated structures are not observed for titrations of a substrate model, displaying only 1:1 complex. These observations allow us to address the question we raised via our kinetic experiments: Why are different behaviors observed for each Lewis acid in the presence of byproduct?

At all equivalents of carbonyl examined with respect to GaCl₃, we observe no additional interaction beyond the formation of a 1:1 Lewis acid-carbonyl complex, consistent with the classical mechanisms drawn for Lewis-acid-mediated reactions. The classical Lewis-acid-mediated model is true for stoichiometric interactions between FeCl₃ and the carbonyls examined (0-1 equiv). However, this model stops being representative of the solution structure of the Lewis acid at superstoichiometric loadings of byproduct carbonyl (>1 equiv). A highly ligated species results when large excesses of byproduct carbonyl are present with respect to FeCl₃. In our study, we examined loadings of carbonyl up to 5 equiv, which would be consistent with a 20 mol% loading of metal halide with respect to carbonyl. With respect to the metathesis reaction, 20 equiv of byproduct are present at the end of a reaction employing 5 mol% catalyst. In the Ga-catalyzed system, 1:1 interactions are all that occur under reaction conditions, suggesting Ga(III) follows the primary cycle of the metathesis reaction (Figure 11), and that byproduct inhibition will arise when the byproduct has a binding affinity for the Lewis acid capable of outcompeting the substrate. Alternatively, the behavior of FeCl₃ changes over the course of the reaction. At low turnovers, the primary cycle efficiently converts substrate **1** to product **2**. However, as the concentration of byproduct increases, the Fe center of 1:1 complex **7** is ligated by additional byproduct carbonyls, forming highly ligated complexes like **28**, outside of the primary cycle. Carbonyl exchange data suggest that at high substrate concentrations relative to **3**, byproduct can be displaced from the complex (Figure 10D). As a result, either substrate can still form **4** by displacing multiple byproduct ligands, or **28** can be converted

to **29**. In the former case, the decrease in [**4**] will lead to a lower turnover frequency. In the case of the secondary cycle, the decreased rate may result from an increase in the degree of coordination to the Lewis acid, which is consistent with the report of Denmark and coworkers who showed that the structure of the Lewis acid-carbonyl complex can affect the reactivity of the carbonyl.²⁰ By attaching the carbonyl to sterically encumbered catalyst **28**, the turnover-limiting [2+2]-cycloaddition becomes more difficult by inhibiting association of the pendant olefin with the carbonyl. This steric inhibition is analogous to the inhibition observed in SmI₂-mediated ketyl-olefin 5-*exo-trig* cyclizations reported by Flowers and coworkers.²¹ Lastly, this result is consistent with our previous observations that the presence of exogenous Lewis bases inhibits product formation.⁸

To test the explanatory power of our model for Lewis acid behavior, we examined a system reported by Schindler and coworkers that produces dihydropyrrole **33** and **13** (Figure 12A).^{4c} This system is analogous to the work of Li and coworkers^{4a} with two key modifications appropriate for the testing of our supposition: 1) the system does not require allyltrimethylsilane to eliminate the byproduct, and 2) the application of the FTs group decreases the likelihood of interaction of this protecting group with the Lewis acid mediator. As a result, these conditions allow us to see the competition between the substrate carbonyl and the byproduct carbonyl.

We examined the FeCl₃-catalyzed system (■, Figure 12B), as well as a GaCl₃-catalyzed system (●, Figure 12B). Intriguingly, GaCl₃ displays an initial rate faster than that of the FeCl₃-mediated reaction, while the FeCl₃ system maintains a higher rate at high conversion of substrate. Next, we initiated the reaction in the presence of 1 equiv **13** with respect to the metal halide. In the presence of added byproduct **13**, a significant decrease in rate occurs for the Fe(III)-mediated system, while no reaction is observed with GaCl₃ even after 4 h. This system requires an order of magnitude more Lewis acid than that of Figure 2, suggesting that substrate **31** has a much lower affinity for each Lewis acid than substrate **15**. This lower relative affinity makes byproduct inhibition significantly more pronounced. Further, this inhibition is so pronounced in the Ga-mediated system that reactivity is prevented, while FeCl₃ is still capable of carrying out the reaction in the presence of 1 equiv **13**. The GaCl₃ result is consistent with direct competition between the substrate and byproduct; whereas, the FeCl₃ reaction is still able to proceed because multiple carbonyls are capable of accessing the metal center.

Lastly, this mechanistic proposal facilitates the adaptation of new procedures by synthetic chemists attempting to employ the metathesis reaction to recalcitrant substrates. The benzaldehyde-producing transformation in Figure 12A is facilitated by an increase in the loading of Lewis acid.^{4c} By increasing the ratio of FeCl₃ to byproduct, the reversible aggregation process favors the 1:1 Lewis acid-carbonyl complex. As a result, the metathesis reaction can remain in the primary cycle until higher conversions of starting material. Alternatively, reports by the Li^{4a} and Schindler^{4c} labs have addressed benzaldehyde-mediated inhibition by the addition of allyltrimethylsilane to chemically remove benzaldehyde from the system. To address acetone-mediated inhibition, a similar increase in the loading of Lewis acid can shift the equilibrium to favor the primary cycle. Alternatively, we have found that increasing reaction temperature can improve turnover of the catalyst.^{4c} For example, the reaction depicted in Figure 2A is performed at 0 °C and reaches completion in about 20 min. When the same reaction is

performed in the presence of 0.5 equiv **3** with respect to substrate at 0 °C, the reaction terminates early. When the **3**-containing system is heated to 40 °C, the reaction reaches full conversion in 20 min.

Conclusion

The solution structures of metathesis-active catalysts were investigated on the basis of kinetic, spectroscopic, colligative, and crystallographic experiments. These data have given us insight into the divergent kinetic behavior of GaCl₃ and FeCl₃ as catalysts in DCE. GaCl₃ interacts with carbonyls through a classical Lewis acid-Lewis base interaction, forming a 1:1 coordination complex, regardless of relative amount of carbonyl. Conversely, FeCl₃ does not only exist as a 1:1 coordination complex when employed as a catalyst, but rather can be reversibly ligated by multiple molecules of byproduct, while potentially remaining catalytically active when substrate-binding affinity is high. The presence of alternative Lewis bases in addition to the substrate carbonyl inhibits the turnover-limiting [2+2]-cycloaddition that yields product. This work describing the solution structures for catalysis of aromatic carbonyls, in concert with the recent report of Fe(III) dimers by Schindler, Sigman, and Zimmerman for the reaction of aliphatic carbonyls,^{4e} indicates that significant consideration of solution structures allows for a more complete understanding of reaction behavior in catalytic systems. Indeed, the highly ligated Fe(III) complexes we describe likely have a more pronounced inhibitory effect on the formation of the superelectrophilic iron dimers, evidenced by the need for elevated temperatures in some cases or the addition of allyltrimethylsilane in benzaldehyde producing substrates. When alternatives to chlorinated solvents are considered, further complications arise, ranging from inhibition of reactivity with Lewis basic solvents⁸ to the trapping of metathesis intermediates in more lipophilic solvents.^{4b,11} We are currently investigating the complexities of solvent interactions to map the diverse array of solution structures. These considerations are not only important for reaction design and catalyst selection, but also for computational analysis of reaction intermediates and transition states. Further, the development of ring-opening and cross carbonyl-olefin metathesis reactions requires the ability of the catalyst to adequately differentiate between substrate and product carbonyls. We have begun studies of other metathesis-active Lewis acids to ascertain the full scope of this effect. Further, the described byproduct inhibition is likely a factor in many carbonyl-based FeCl₃-catalyzed reactions beyond carbonyl-olefin metathesis. We are currently examining alternative systems to understand the impact of the solution structures accessible to FeCl₃ in catalytic regimes.

ASSOCIATED CONTENT

Supporting Information

The Supporting Information is available free of charge on the ACS Publications website.

Experimental data (PDF)
Data for C₂₈H₂₄O₄Fe₂Cl₆ (CIF)

AUTHOR INFORMATION

Corresponding Author

* jdevery@luc.edu

ORCID

Carly S. Hanson: 0000-0002-4288-1219
James J. Devery, III: 0000-0003-3124-465X

Notes

The authors declare no competing financial interest.

ACKNOWLEDGMENT

We thank Loyola University Chicago, Merck & Co., Inc., and the NIH/National Institute of General Medical Sciences (GM128126) for financial support. This work made use of the Jerome B. Cohen X-Ray Diffraction Facility supported by the MRSEC program of the National Science Foundation (DMR-1720139) at the Materials Research Center of Northwestern University and the Soft and Hybrid Nanotechnology Experimental (SHyNE) Resource (NSF ECCS-1542205). We are very grateful to Prof. Wei-Tsung Lee, Ms. Adriana Lugosan, Mrs. Loretta Devery, and Mr. James Devery for helpful discussions and suggestions. We also thank the reviewers for their insightful comments on an earlier version of this paper.

REFERENCES

- (1) a) *NATO ASI Series, Ser. C: Mathematical and Physical Sciences: Selectivities in Lewis Acid Promoted Reactions*, Kluwer, 1989, vol. 289. b) Santelli, M.; Pons, J.-M. *Lewis Acids and Selectivity in Organic Synthesis*, CRC Press, Boca Raton, 1996. c) Yamamoto, H. Ed., *Lewis Acids in Organic Synthesis*, Wiley-VCH, Weinheim; New York, 2000. d) Satchell, D. P. N.; Satchell, R. S. Quantitative Aspects of the Lewis Acidity of Covalent Metal Halides and Their Organo Derivatives. *Chem. Rev.*, **1969**, *69*, 251–278.
- (2) a) Ludwig, J. R.; Schindler, C. S. Lewis Acid Catalyzed Carbonyl-Olefin Metathesis. *Synlett*, **2017**, *28*, 1501–1509. b) Becker, M. R.; Watson, R. B.; Schindler, C. S. Beyond Olefins: New Metathesis Directions for Synthesis. *Chem. Soc. Rev.*, **2018**, *47*, 7867–7881.
- (3) Ludwig, J. R.; Zimmerman, P. M.; Gianino J. B.; Schindler, C. S. Iron(III)-Catalyzed Carbonyl-Olefin Metathesis. *Nature*, **2016**, *533*, 374–379.
- (4) a) Ma, L.; Li, W.; Xi, H.; Bai, X.; Ma, E.; Yan, X.; Li, Z. FeCl₃-Catalyzed Ring-Closing Carbonyl-Olefin Metathesis. *Angew. Chem. Int. Ed.*, **2016**, *55*, 10410–10413. b) McAtee, C. C.; Riehl, P. S.; Schindler, C. S. Polycyclic Aromatic Hydrocarbons via Iron(III)-Catalyzed Carbonyl-Olefin Metathesis. *J. Am. Chem. Soc.*, **2017**, *139*, 2960–2963. c) Groso, E. J.; Golonka, A. N.; Harding, R. A.; Alexander, B. W.; Sodano T. M.; Schindler, C. S. 3-Aryl-2,5-Dihydropyroles via Catalytic Carbonyl-Olefin Metathesis. *ACS Catal.*, **2018**, *8*, 2006–2011. d) Ludwig, J. R.; Watson, R. B.; Nasrallah, D. J.; Gianino, J. B.; Zimmerman, P. M.; Wiscons, R. A.; Schindler, C. S. Interrupted Carbonyl-Olefin Metathesis via Oxygen Atom Transfer. *Science*, **2018**, *361*, 1363–1369. e) Albright, H.; Riehl, P. S.; McAtee, C. C.; Reid, J. P.; Ludwig, J. R.; Karp, L. A.; Zimmerman, P. M.; Sigman, M. S.; Schindler, C. S. Catalytic Carbonyl-Olefin Metathesis of Aliphatic Ketones: Iron(III) Homo-Dimers as Lewis Acidic Superelectrophiles. *J. Am. Chem. Soc.* **2019**, *141*, 1690–1700.
- (5) Albright, H.; Vonesh, H. L.; Becker, M. R.; Alexander, B. W.; Ludwig, J. R.; Wiscons, R. A.; Schindler, C. S. GaCl₃-Catalyzed Ring-Opening Carbonyl-Olefin Metathesis. *Org. Lett.*, **2018**, *20*, 4954–4958.
- (6) Tran, U. P. N.; Oss, G.; Breugst, M.; Detmar, E.; Pace, D. P.; Liyanto, K.; Nguyen, T. V. Carbonyl-Olefin Metathesis Catalyzed by Molecular Iodine. *ACS Catal.* **2019**, *9*, 912–919.
- (7) a) Catti, L.; Tiefenbacher, K. Brønsted Acid-Catalyzed Carbonyl-Olefin Metathesis inside a Self-Assembled Supramolecular Host. *Angew. Chem. Int. Ed.*, **2018**, *57*, 14589–14592. b) Tran, U. P. N.; Oss, G.; Pace, D. P.; Ho J.; Nguyen, T. V. Tropylium-Promoted Carbonyl-Olefin Metathesis Reactions. *Chem. Sci.*, **2018**, *9*, 5145–5151.
- (8) Ludwig, J. R.; Phan, S.; McAtee, C. C.; Zimmerman, P. M.; Devery, J. J., III; Schindler, C. S. Mechanistic Investigations of the Iron(III)-Catalyzed Carbonyl-Olefin Metathesis Reaction. *J. Am. Chem. Soc.*, **2017**, *139*, 10832–10842.
- (9) Hosomi, A.; Sakurai, H. Syntheses of γ,δ -Unsaturated Alcohols from Allylsilanes and Carbonyl Compounds in the Presence of Titanium Tetrachloride. *Tetrahedron Lett.*, **1976**, *17*, 1295–1298.

(10) Becker, M. R.; Rykaczewski, K. A.; Ludwig, J. R.; Schindler, C. S. Carbonyl-Olefin Metathesis for the Synthesis of Cyclic Olefins. *Org. Synth.*, **2018**, *95*, 472–485.

(11) See Supporting Information for more details.

(12) a) Mohammad, A.; Satchell, D. P. N.; Satchell, R. S. Quantitative Aspects of Lewis Acidity. Part VIII. The Validity of Infrared Carbonyl Shifts as Measures of Lewis Acid Strength. The Interaction of Lewis Acids and Phenalen-1-one(perinaphthenone). *J. Chem. Soc. B Phys. Org.*, **1967**, 723–725. b) Satchell, D. P. N.; Satchell, R. S. Quantitative Aspects of Lewis Acidity. *Q. Rev. Chem. Soc.*, **1971**, *25*, 171–199. c) Driessen, W. L.; Groeneveld, W. L. Complexes with Ligands Containing the Carbonyl Group. Part I: Complexes with Acetone of Some Divalent Metals Containing Tetrachloro-ferrate(III) and -In-date(III) Anions. *Recl. Trav. Chim. Pays-Bas*, **1969**, *88*, 977–988. d) Driessen, W. L.; Groeneveld, W. L. Complexes with Ligands Containing the Carbonyl Group. Part III: Metal (II) Acetaldehyde, Propionaldehyde and Benzaldehyde Solvates. *Recl. Trav. Chim. Pays-Bas*, **1971**, *90*, 87–96. e) Driessen, W. L.; Groeneveld, W. L. Complexes with Ligands Containing the Carbonyl Group. Part IV Metal(II) Butanone, Acetophenone, and Chloroacetone Solvates. *Recl. Trav. Chim. Pays-Bas*, **1971**, *90*, 258–264.

(13) Susz, B. P.; Cooke, I. Etude du Spectre Infrarouge de Complexes Formés par les Halogénures d'Aluminium. I. Complexes de l'Acétophénone et de la Benzophénone; Comparaison avec les Spectres de Divers Composés Organiques Présentant la Liaison Aluminium-oxygène. *Helv. Chim. Acta*, **1954**, *37*, 1273–1280.

(14) a) Susz, B. P.; Lachavanne, A. Etude de Composés d'Addition des Acides de Lewis. V. Absorption Infrarouge de Composés d'Addition Formés par le Chlorure de Titane avec la Benzophénone et l'Acétophénone. *Helv. Chim. Acta*, **1958**, *41*, 634–636. b) Cassimatis, D.; Susz, B. P. Etude des Composés d'Addition des Acides de LEWIS. XI. Spectre d'Absorption Infrarouge du Composé d'Addition CH₃COCH₃, TiCl₄. *Helv. Chim. Acta*, **1960**, *43*, 852–862. c) Weber, R.; Susz, B. P. Etude des Composés d'Addition des Acides de Lewis XXX. Note Préliminaire Sur les Composés d'Addition Entre Aldéhydes et TiCl₄. *Helv. Chim. Acta*, **1967**, *50*, 2226–2232.

(15) a) Chalandon, P.; Susz, B. P. Etude de Composés d'Addition des Acides de Lewis. VI Spectre d'Absorption Infrarouge de l'Acétone-trifluorure de Bore; Apectre d'Absorption Infrarouge et Moment de Dipôle du Di-propyl-cétone-trifluorure de Bore. *Helv. Chim. Acta*, **1958**, *41*, 697–704. b) Susz B. P.; Chalandon, P. Etude de Composés d'Addition des Acides de Lewis. IX. - Spectres d'Absorption Infrarouge des Composés Formés par la Benzophénone et l'Acétophénone avec

BF₃, FeCl₃, ZnCl₂ et AlCl₃ et Nature de la Liaison Oxygène-métal. *Helv. Chim. Acta*, **1958**, *41*, 1332–1341.

(16) a) Greenwood, N. N. The Ionic Properties and Thermochemistry of Addition Compounds of Gallium Trichloride and Tribromide. *J. Inorg. Nucl. Chem.*, **1958**, *8*, 234–240. b) Greenwood, N. N.; Perkins, P. G. 68. Thermochemistry of the Systems Which Boron Trichloride and Gallium Trichloride Form with Acetone and Acetyl Chloride, and the Heat of Solution of Boron Tribromide in Acetone. *J. Chem. Soc.*, **1960**, 356.

(17) Davlieva, M. G.; Lindeman, S. V.; Neretin, I. S.; Kochi, J. K. Isolation, X-ray Structures, and Electronic Spectra of Reactive Intermediates in Friedel–Crafts Acylations. *J. Org. Chem.*, **2005**, *70*, 4013–4021.

(18) a) Novikov, R. A.; Potapov, K. V.; Chistikov, D. N.; Tarasova, A. V.; Grigoriev, M. S.; Timofeev, V. P.; Tomilov, Y. V. Synthesis and Structures of Cyclopropanedicarboxylate Gallium Complexes. *Organometallics*, **2015**, *34*, 4238–4250. b) Novikov, R. A.; Denisov, D. A.; Potapov, K. V.; Tkachev, Y. V.; Shulishov, E. V.; Tomilov, Y. V. Ionic Ga-Complexes of Alkylidene- and Arylmethylidenemalonates and Their Reactions with Acetylenes: An In-Depth Look into the Mechanism of the Occurring Gallium Chemistry. *J. Am. Chem. Soc.*, **2018**, *140*, 14381–14390.

(19) For a review of solid state structures of Lewis acids and carbonyls: Shambayati, S.; Crowe, W. E.; Schreiber, S. L. On the Conformation and Structure of Organometal Complexes in the Solid State: Two Studies Relevant to Chemical Synthesis. *Angew. Chem. Int. Ed.*, **1990**, *29*, 256–272.

(20) a) Denmark, S. E.; Henke, B. R.; Weber, E. SnCl₄(4-tert-BuC₆H₄CHO)₂. X-ray Crystal Structure, Solution NMR, and Implications for Reactions at Complexed Carbonyls. *J. Am. Chem. Soc.*, **1987**, *109*, 2512–2514. b) Denmark, S. E.; Almstead, N. G. Spectroscopic Studies on the Structure and Conformation of Lewis Acid-Aldehyde Complexes. *J. Am. Chem. Soc.*, **1993**, *115*, 3133–3139.

(21) Sadasivam, D. V.; Antharjanam, P. K. S.; Prasad E.; Flowers, R. A., II Mechanistic Study of Samarium Diiodide-HMPA Initiated 5-exo-trig Ketyl–Olefin Coupling: The Role of HMPA in Post-Electron Transfer Steps. *J. Am. Chem. Soc.*, **2008**, *130*, 7228–7229.

